ORIGINAL RESEARCH

Density and Time Characteristics of CSF-venous fistulas on CT myelography in Patients with Spontaneous Intracranial Hypotension

Diogo G.L. Edelmuth, Timothy J. Amrhein, and Peter G. Kranz

ABSTRACT

BACKGROUND AND PURPOSE: The conspicuity of CSF-venous fistulas (CVF) on specialized myelographic imaging protocols varies, and the factors that determine their visibility have not yet been extensively studied. The purpose of this study was to determine the relative effect of two variables on CVF visibility: timing of imaging and intrathecal contrast density.

MATERIALS AND METHODS: Retrospective cohort of 24 patients with spontaneous intracranial hypotension due to a CVF who underwent a total of 34 CT myelographies. All CTM acquisitions that included the level of the known definite CVF were evaluated for (1) time passed after injection of contrast, (2) attenuation of the adjacent subarachnoid space, (3) subjective visibility of the CVF on that series,(4) attenuation of the corresponding draining vein and (5) contrast dose used.

RESULTS: A total of 131 acquisitions included the level of the known CVFs. Attenuation values of the thecal sac were significantly higher in acquisitions where the CVFs were definitely visible (average 2283 HU) than on acquisitions where the CVFs were equivocal or not visible (764 HU and 583 HU respectively). No significant difference was shown in the timing of the acquisitions between the three groups (12.8 min, 20.4 min and 17.5 min respectively). Multivariate linear regression showed thecal sac density to be the only independent predictor of the density of the CVF draining vein, while time passed after contrast injection was not independently correlated.

CONCLUSIONS: Intrathecal contrast density has a strong positive relationship with the visibility of CVF. Timing of the acquisition was not an independent predictor of CVF visibility under our acquisition protocol

ABBREVIATIONS: LDCTM = lateral decubitus CT myelography; CVF = CSF-venous fistula; IOCM = iodinated contrast media

Received month day, year; accepted after revision month day, year.
From the Department of Radiology and Oncology of Hospital das Clínicas da Faculdade de Medicina da Universidade de São Paulo, São Paulo, Brazil (D.G.L.E.), Departamento de Radiologia e Centro de Medicina Intervencionista, Hospital Israelita Albert Einstein, São Paulo, São Paulo, Brazil (D.G.L.E.), Hospital Sírio-Libanês, São Paulo, São Paulo, Brazil (D.G.L.E.) and Duke University Medical Center, Durham, NC, United States of America (T.J.A., P.G.K.).

The authors declare no conflicts of interest related to the content of this article.

Please address correspondence to Diogo G.L. Edelmuth, MD, Department of Radiology and Oncology of Hospital das Clínicas da Faculdade de Medicina da Universidade de São Paulo, Travessa da, R. Dr. Ovídio Pires de Campos, 75, São Paulo, São Paulo 05403-010, Brazil; diogo.e@hc.fm.usp.br.

SUMMARY SECTION

PREVIOUS LITERATURE: Previously described factors associated with CVF conspicuity on myelographic examinations include timing of acquisition, patient position and breathing phase. Attenuation of the thecal sac at the level of the CVF has not been specifically studied as an independent determinant of diagnostic yield.

KEY FINDINGS: Intrathecal contrast density has a strong positive relationship with CVF conspicuity and was the only independent predictor in this series, whereas timing of acquisition, contrast dose and patient position were not independently related to CVF visibility.

KNOWLEDGE ADVANCEMENT: Some factors previously known to be related to CVF visibility on myelographic examinations, such as decubitus positioning and early acquisitions, might be deriving this increased yield mostly because of increased contrast density at the fistulous site.

INTRODUCTION

CSF-venous fistulas (CVFs) are a frequent cause of spontaneous intracranial hypotension1. Lateral decubitus CT myelography (LDCTM) and lateral decubitus digital subtraction myelography (DSM) are the main studies used to the detection of the exact site of CVF[1–4]. Their diagnosis depends on very specific acquisition protocols, which had in the past led to a great number of false negative conventional CT myelography studies. More recently, refinements in technique have resulted in increased diagnostic accuracy, with some referral centers reporting positive yields of 70%-100% for patients with a high suspicion based on brain MR findings[5–7]. However, false-negative studies still occur, and detection of CVFs remains challenging in practice. Understanding the factors that increase the conspicuity of CVFs is therefore important to optimize myelographic protocols. Some authors have emphasized that immediate scanning after contrast

injection is needed, however the techniques utilized in these reports have typically involved dynamic protocols where contrast is or may be actively flowing in the thecal sac, and thus contrast density is also changing simultaneously with time[8,9]. As a result, the independent effects of timing and contrast density are difficult to discern from these studies.

The purpose of this study was to determine the relative effect of two variables on CVF visibility: timing of imaging and intrathecal contrast density. Secondarily, we sought to determine whether threshold values for intrathecal contrast attenuation could be established that were associated with higher rates of CVF visualization.

MATERIALS AND METHODS

This investigation is a single-center retrospective cohort study of CTM examinations performed in SIH patients meeting ICHD-3 criteria[10] between December 2022 and July 2024 in a tertiary center in Brazil. Methodology of STROBE was followed.

Inclusion criteria were: (1) any CTM acquisition that included the level of a known CVF; (2) any CTM exam protocol (i.e. conventional, ultrafast/dynamic and decubitus); (3) patient had a definite CVF in at least one of their CTM. Exclusion criteria were: (1) acquisition did not include the level of the known CVF; (2) the patient received targeted treatment prior to the current study/acquisition (unless the current study showed definite persistence or recurrence of the CVF); (3) patients with equivocal diagnosis of the CVF in all available studies (as per the revision of images and reclassification of this study, described further in "Technical evaluation").

Myelography technique

Examinations were performed under one of the three following protocols: (1) conventional[11], which was defined as only delayed images with homogeneous distribution of contrast within the thecal sac (regardless of patient position, which could include decubitus); (2) ultrafast/dynamic[5,12–14], consisting of image acquisition during or immediately after the injection of contrast and patient on decubitus Trendelenburg position; or (3) static decubitus[6,15,16], with elevation of the head and hips and a static pool of dense contrast layering over the lateral portion of the thecal sac. Examinations were all performed after the injection of either 10 or 20 ml of contrast media (Visipaque 320, GE), according to the discretion of the proceduralist. Lumbar puncture and contrast injection were performed under CT guidance (Siemens Somatom AS) in all cases, performed by one of 5 different proceduralists. Lumbar puncture was performed from L2-L3 to L5-S1, without any standardized preference. Saline pressurization was not performed.

Technical evaluation

For each CTM acquisition, quantitative analysis of the intrathecal contrast density was performed by a musculoskeletal radiologist with 5 years post-fellowship experience in performing and interpreting CTM (DGLE). This was performed at the level of the known CVF, even if the CVF was not visible on that specific acquisition (but was visible on a previous or subsequent acquisition), by measuring the mean attenuation value using a standardized 0.05 cm^2 ROI immediately caudal to the dural emergence of the corresponding nerve root, within the most lateral part of the thecal sac, similar to previously published literature[16]. Supplementary figure 3 shows the technique used for this measurement.

Time between the injection of contrast and image acquisition in minutes was also recorded. For conventional and decubitus CTM protocols, this was performed by subtracting the DICOM timestamp on the CT-fluoroscopy image during the injection of contrast from that of the specific acquisition under evaluation. For dynamic/ultrafast protocols, which have the first image acquired immediately during the injection of contrast, the time was designated as 1 minute to represent the lowest possible time interval.

For each CTM acquisition, the subjective conspicuity of the CVF was characterized as (1) definite, when it was thought that the diagnosis of a CVF could be easily and definitely made based on that series alone; (2) equivocal, when a suspicious image was seen for a CVF, but the diagnostic confidence was low; or (3) not visible. Objective quantitative evaluation of the CVF was performed by measuring the density of its draining vein with a 0.005 cm^2 ROI on the most conspicuous site of venous contrast uptake. If the CVF was not visible on that acquisition, then the measurement was performed over a vein known to be a draining vein based on the acquisition where the CVF was visible. Both the subjective and the objective assessments of the veins were done by the same radiologist who performed the thecal sac measurements. Diagnostic acquisitions were all performed with 120 KeV peak, including the few outside examinations considered. Measurements were performed under soft tissue kernel reconstructions.

We sought to determine a threshold of minimal contrast density that ensures a good diagnostic sensitivity. For the purpose of having a binary outcome for this question, acquisitions were considered either positive or negative, and both definite and equivocal acquisitions were grouped as positive, as in both cases a CVF could be suspected.

Statistical analysis

Image acquisitions were grouped according to the visibility of the CVF (definite, equivocal and not visible) and were compared relative to attenuation in the adjacent thecal sac, time to imaging after intrathecal contrast injection, the position of the patient (i.e. whether the CVF was on the dependent side of the thecal sac or not) and contrast dose (i.e. 10 ml or 20 ml). ANOVA tests were performed to assess statistical significance between the difference in means of the quantitative values (time and sac density). A Pearson's Chi-squared test was performed to test for statistical significance of the difference in visibility of the CVF depending on the patient position. A student's T test was used to compare the thecal sac attenuation between patient positions and contrast doses. Multivariate linear regression analysis was performed to check whether these same parameters (time, thecal sac contrast density and patient position) were independent predictors of the density of the CVF draining vein. Logistic regression was used to find the best threshold for thecal sac density that separated positive from negative acquisitions, and other reasonable thresholds were explored to maximize diagnostic yield. A p value < 0.05 was considered statistically significant.

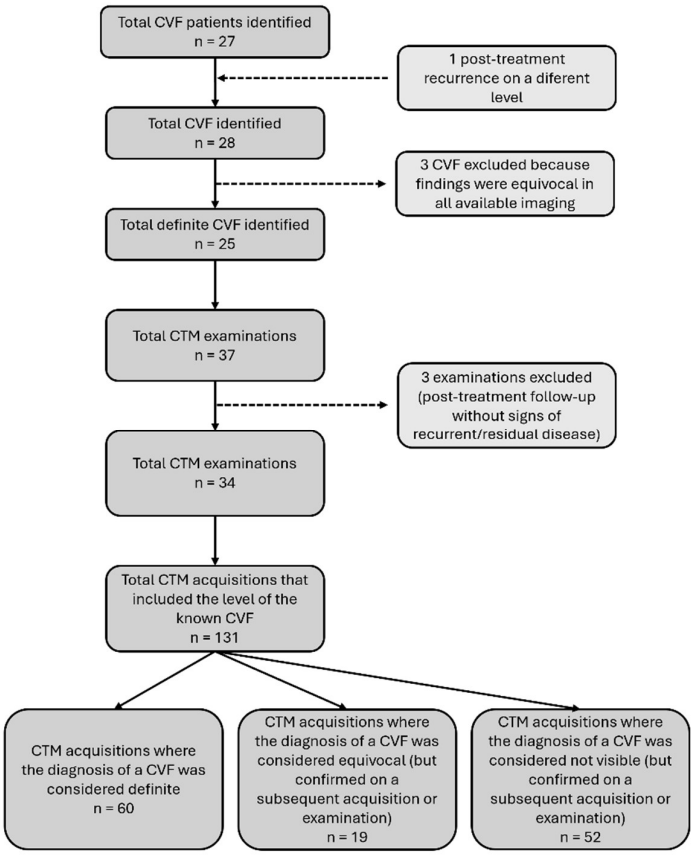

FIG 1. Flowchart of case selection.

RESULTS

A total of 28 fistulas were diagnosed in 27 patients in the studied period (one patient had a recurrence on a new different level). Upon review, three CVFs were considered equivocal on all available imaging exams and were excluded, resulting in 25 remaining definite CVF in 24 different patients. These patients were evaluated with a total of 37 different CTMs. Three examinations in 3 different patients were excluded, because they represented post-treatment follow-ups with no signs of persistent/recurrent fistula. From the remaining 34 examinations, a total of 131 CTM acquisitions included the level of the known fistula and were reviewed (Figure 1).

Reasons for more than one CTM per patient consisted of: conventional examinations from an outside hospital prior to referral (3 patients), post-treatment evaluation of recurrence with definite signs of persistent CVF (5 patients) or follow-up evaluation of a suspicious but indefinite finding on the first CTM (1 patient). Each patient had an average of 1.8 CTMs (median = 1, range = 1 - 4, SD = 1.9).

Relative to the acquisition protocols, there were 5 conventional CTMs (21 acquisitions, mean of 4.2 acquisitions per exam, SD = 2.6), 4 dynamic/ultrafast CTMs (13 acquisitions, mean of 3.6 acquisitions per exam, SD = 1.0) and 25 static decubitus CTMs (97 acquisitions, mean of 3.9 acquisitions per exam, SD = 1.7). Table 1 summarizes the descriptive data of the results.

For proven CVFs analyzed (either on the assessed CTM or a subsequent follow-up CTM), average attenuation of the thecal sac was 2283 HU (SD = 900 HU) adjacent to CVFs that were definitely visible on that series, 764 HU (SD = 641 HU) when the acquisition produced indefinite findings, and 548 HU (SD = 549 HU) when the known CVF was not visible on the series. There was a statistically significant difference in attenuation values between the first group where CVFs were definitely visible and the two other groups ($p<0.001$). Figure 2A illustrates the distribution of acquisitions relative to the thecal sac density. Figure 3 illustrates the difference in medians/distributions. Supplementary figure l shows this same relationship when only acquisitions in ipsilateral decubitus are considered.

The average time from contrast injection to the image acquisition in these same three groups were 12.8 min, 20.4 min and 17.5 min, respectively, which did not represent a statistically significant difference ($p = 0.11$). Figure 2B illustrates the distribution of acquisitions relative to the time to imaging after intrathecal contrast injection.

CVFs were 4.8 (95% CI 2.7 – 8.6) times more likely to be definitely visible in acquisitions where the patient was positioned decubitus ipsilateral to the side of the CVF ($p<0.001$) (Table 2). Average thecal sac attenuation at the site of the CVF was also much higher when the patient was placed with the CVF on the dependent side of the thecal sac (2164 HU [SD = 1026] versus 534 HU [SD = 340]; $p<0.001$) when considering all acquisitions.

Average thecal sac attenuation at the site of the CVF was higher in acquisitions that followed the injection of 20 ml of contrast compared to 10 ml (1470 HU versus 1021 HU; $p = 0.03$). CVFs were slightly more likely to be definitely visible in acquisitions following 20 ml of

contrast, but this did not reach statistical significance (OR 1.9 CI 0.8 – 4.4; p = 0.14) (Table 3).

Multivariate regression analysis showed a statistically significant and independent relationship between the density of the thecal sac and the density of the draining vein of the CVF (p < 0.001). Time to imaging after intrathecal contrast injection and dose of injected contrast were not found to be independent predictors (p = 0.28 and p = 0.16 respectively). Even though patient position (side facing down) had a marked relationship with the objective density of the of the CVF draining vein, this did not represent an independent predictor when corrected for the density of the thecal sac in the multivariate analysis (p = 0.39). These data are illustrated in figure 4. Supplementary figure 2 shows this same relationship when only acquisitions in ipsilateral decubitus are considered.

Logistic regression analysis determined a best predictor model for distinguishing positive from negative acquisitions with a threshold of thecal sac contrast density at 820 HU (p < 0.001). Acquisitions above this threshold had a false negative rate of 12%. At a threshold of 1000 HU, the false negative rate decreased to 7%, and, at a threshold of 2000 HU, the false negative rate dropped further to 5%. False negative rates of 67% and 69% were observed for the acquisitions under 1000 HU and 841 HU, respectively. Figures 5, 6 and 7 include sample images of definite, equivocal and not visible (false negative) acquisitions.

Table 1. Overall characteristics of the acquisitions studied.

Scan protocol	Static Decubitus	Ultrafast/ dynamic	Conventional	Total
Exams (n)	25	4	5	34
Acquisitions (n)	97	13	21	131
Sac attenuation (HU)	1531	1415	583	1368
CVF side down	2352	1736	739	2164
Other side down	542	344	547	534
Time after injection (min)	15.2	5	24.8	15.8
CVF				
C7-T1	1			
T1-T2	2			
T2-T3	1			
T5-T6	3			
T6-T7	4			
T7-T8	3			
T8-T9	3			
T9-T10	1			
T10-T11	7			
T11-T12	1			
Right-sided	16 (67%)			
CVF Visibility	Definite	Equivocal	Not visible	
Acquisitions (n)	60	19	52	
Vein (HU)	639	198	5	
Sac (HU)	2282	751	538	

Table 2. Contingency table of CVF visibility relative to patient position during the acquisition.

	Definite	Equivocal	Not visible
Same side as CVF facing down	50	5	12
Other side facing down	10	14	40

Relative rate of definite CVF 4.8 (95% CI 2.7 – 8.6) higher when CVF facing down (P<0.001)

Counts represent acquisitions, not patients.

Table 3. Contingency table of CVF visibility relative to intrathecal contrast dose.

	Definite	Equivocal	Not visible
20 ml	50	17	34
10 ml	10	2	18

Relative rate of definite CVF 1.9 (95% CI 0.8 – 4.4) higher when CVF facing down (P=0.14)
Counts represent acquisitions, not patients.

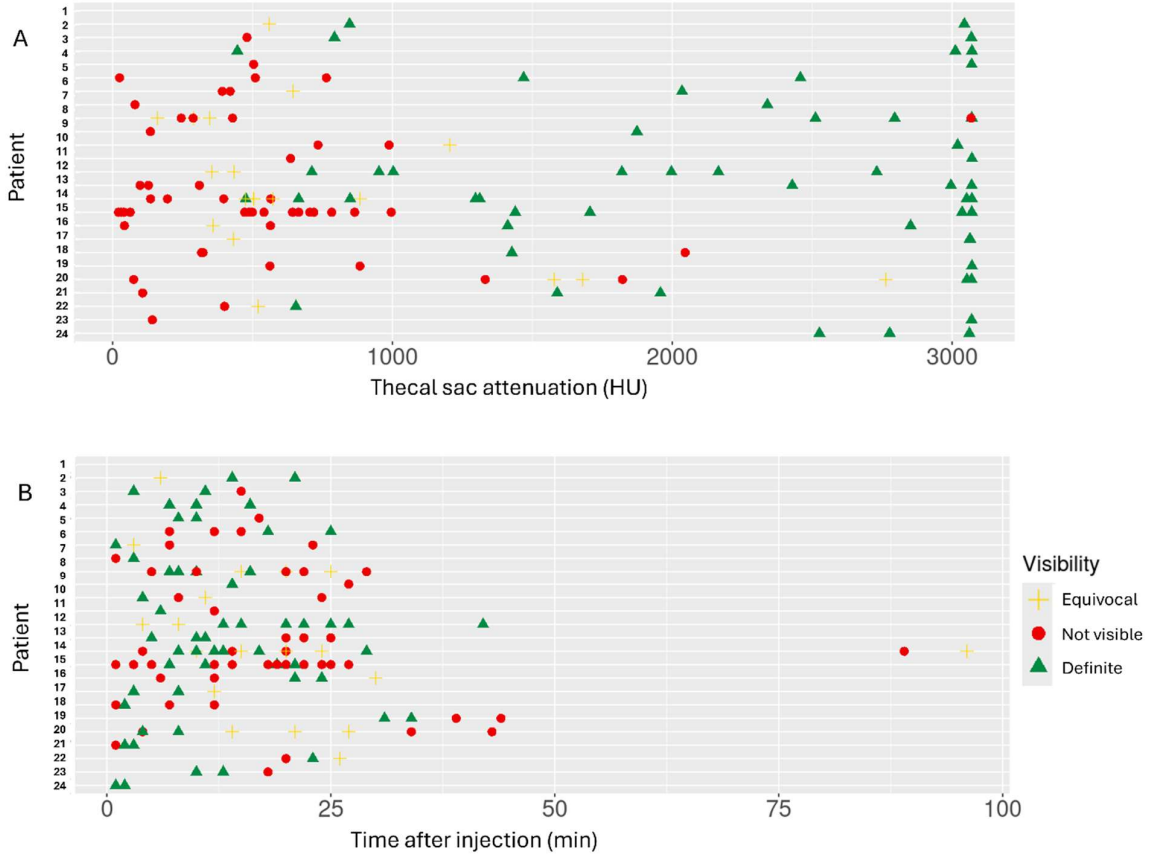

FIG 2. Each row in A and B represents a single patient. Each dot represents a CTM acquisition. In A, the x axis denotes the thecal sac attenuation on the level of a known CVF. In B, the x axis denotes the time passed between contrast injection and the acquisition. Colors represent the subjective visibility of the CVF on that acquisition.

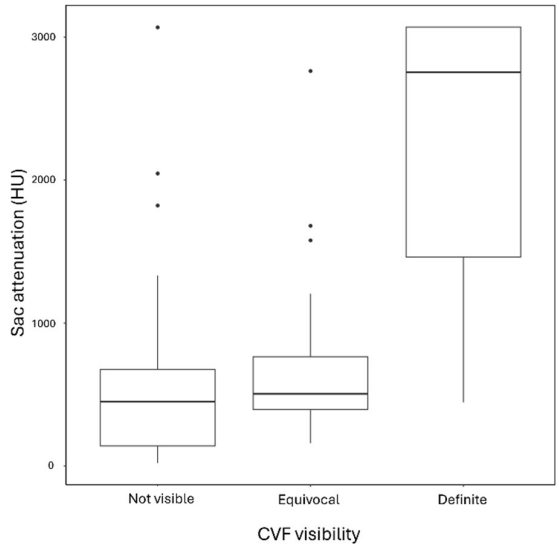

FIG 3. Boxplot graph showing the distribution of thecal sac contrast density in each group of CVF visibility. The group with visible CVF showed a marked and statistically significant higher mean density than the other two groups.Flowchart of case selection.

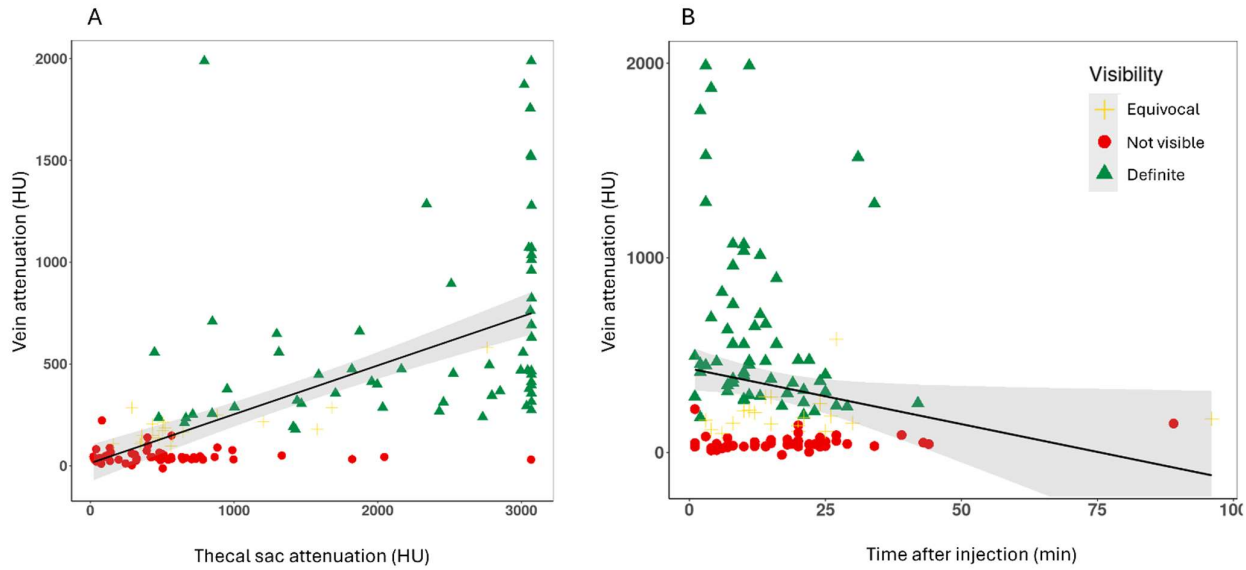

FIG 4. The y axis in both images represents the density of the draining vein of the known CVF. Each dot represents a CTM acquisition. Colors represent the subjective visibility of the CVF on that acquisition. In A, the x axis denotes the thecal sac attenuation on the level of a known CVF, with a statistically significant relationship, even after multivariate regression analysis correcting for time and position. In B, the x axis denotes the time passed between contrast injection and the acquisition, without a significant relationship to the density of the vein, before and after multivariate regression correction.

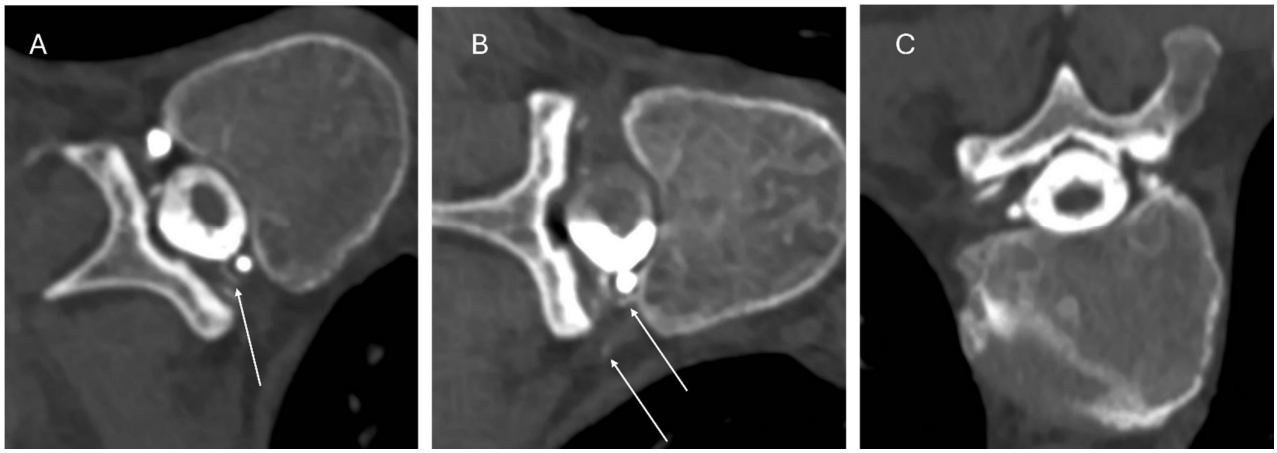

FIG 5. Axial images from different acquisitions during two separate CTMs at the level of a confirmed CVF in an SIH patient. A: left static decubitus CTM with indefinite but suspicious finding for a CVF in the T10-T11 left epidural venous plexus (thecal sac density: 1578 HU, vein density: 180 HU, time passed: 21 min). As an isolated image, it could also represent the dural emergence of the dorsal nerve root. B: left static decubitus CTM with a definitive CVF in the left T10-T11 foramen, represented by multiple epidural, foraminal and extraforaminal vessels opacifying by contrast (thecal sac density: 3070 HU, vein density: 692 HU, time passed: 4 min). C: prone acquisition after static decubitus CTM without any recognizable venous opacification (thecal sac density: 1332HU, vein density: 43 HU, time passed: 51 min).

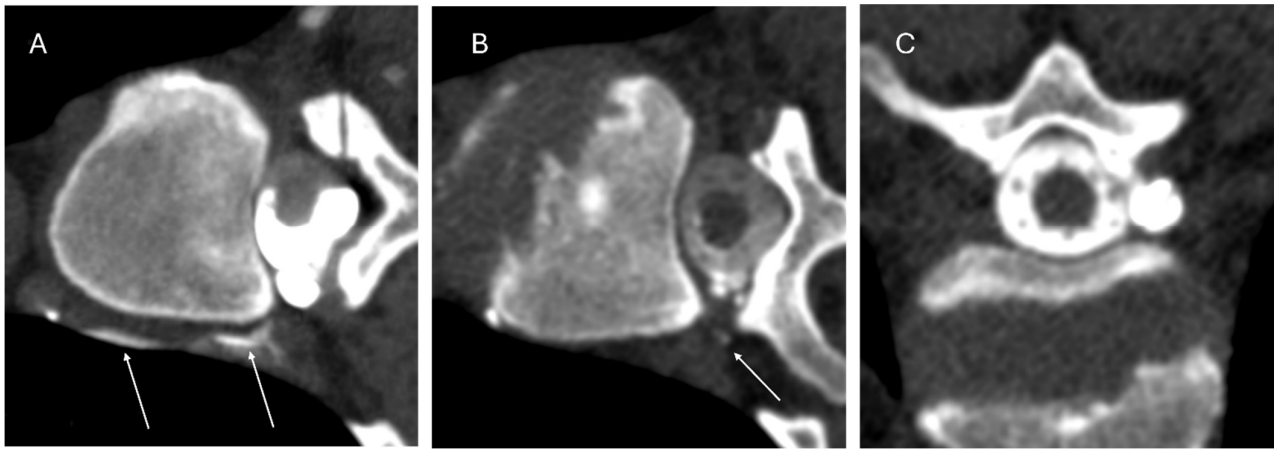

FIG 6. Axial images from different acquisitions during a single CTM at the level of a confirmed CVF in an SIH patient. A: right static decubitus CTM with a definite right T11-T12 CVF draining to the paraspinal vein (thecal sac density: 3020 HU, vein density: 1871 HU, time passed: 4 min). B: right static decubitus CTM with an equivocal finding for a CVF represented by a single faint contrast uptake apparently separate from the nerve root sleeve and diverticle (thecal sac density: 685 HU, vein density: 217 HU, time passed: 8 min). C: prone acquisition after static decubitus CTM without any recognizable venous opacification (thecal sac density: 988 HU, vein density: 77 HU, time passed: 24 min).

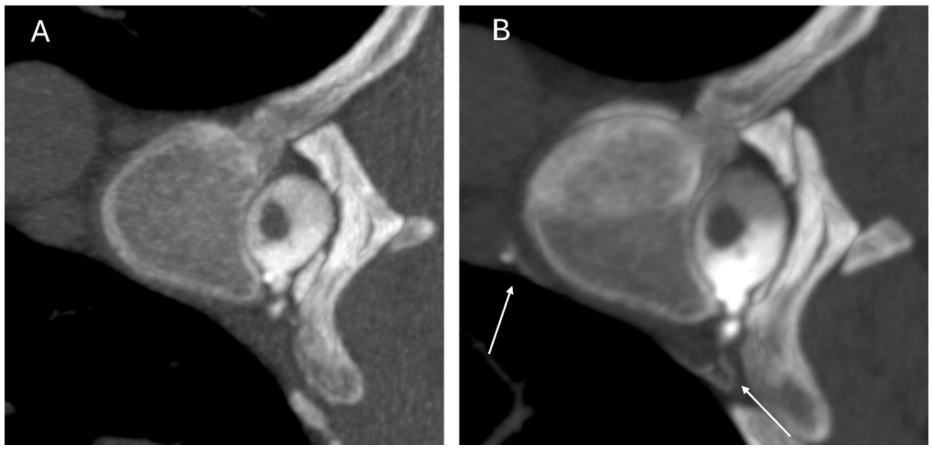

FIG 7. Axial 5.7 mm maximum intensity projection images from two different acquisitions during a single CTM at the level of a confirmed CVF in an SIH patient. A: right static decubitus CTM at the T7-T8 level without any recognizable venous opacification (thecal sac density: 996 HU, vein density: 32 HU, time passed: 12 min). B: right static decubitus CTM with a definite right T7-T8 CVF draining to the paraspinal vein (thecal sac density: 1439 HU, vein density: 321 HU, time passed: 21 min).

DISCUSSION

We have demonstrated a clear relationship between the density of the contrast within the lateral portion of the thecal sac and both the subjective conspicuity as well as the objective density of CVFs. Having the patient in the decubitus position ipsilateral to the CVF also improved visibility of the CVF as well as the density of the corresponding draining vein, however this did not represent an independent predictor in the multivariate analysis. As a result, this suggests that contrast density within the thecal sac is the primary driver of CVF conspicuity, as it remained the only independent predictor among the parameters analyzed in this study. Furthermore, we have also demonstrated that interval after intrathecal contrast injection was not a predictor of the visibility of CVF, either in the univariate or multivariate analysis.

Two papers have previously studied the time characteristics of the conspicuity of CVF[8,9]. The first one evaluated cases under digital subtraction myelography (DSM), reporting a mean time of 9 seconds from the moment contrast reaches the CVF level to the actual appearance of the CVF on imaging, and a mean duration of appearance of 50 seconds[8]. Although this reported timeframe differs greatly from the one presented in our paper (average of 13 minutes for acquisitions with a definite CVF visible), the difference in technique between both studies can easily account for the disparity. On DSM, patients are positioned on lateral Trendelenburg position, and contrast continuously flows cranially as time passes, with the bulk of the contrast density moving away from the site of the fistula over the first 1-2 minutes[17]. In DSM, therefore, density of contrast in the thecal sac changes as a function of time, initially rising, then falling again as the bolus passes, such that these variables are not independent of each other. Static imaging independent of time is more difficult with fluoroscopy-based techniques, as the continuous/dynamic cranial flow of contrast is required for DSM, as it involves subtraction of the mask image from the myelographic image. Respiration must be suspended during the interval between mask and myelographic acquisition to avoid misregistration artifact, necessitating a rapid acquisition of images, which impedes the use of static imaging. Further, because contrast density is easier to quantitatively measure on CT than on fluoroscopy, CTM may be better suited for considering time and contrast density independently.

In the second study[9], the authors utilized CTM and reported varying and unpredictable conspicuity of CVF over 1-3 acquisitions with the patient on decubitus position. Although the authors did not specify the exact time of these acquisitions relative to the injection of contrast, the protocol described immediate scanning after decubitus Trendelenburg positioning, when contrast density and distribution could have been changing in the thecal sac. This study did not evaluate the contrast density within the thecal sac as an independent variable for each acquisition where the CVF visibility was evaluated. If contrast density changed between acquisitions in the dynamic protocol described by the authors (with density thus being a function of time), one would not be able to assess whether density or time had a greater influence on CVF conspicuity. For this reason, in our study, we assessed the impact of both contrast density and time on CVF conspicuity, using both static and dynamic techniques. Further, the technique used by the authors of the prior study potentially could have resulted in lower total intrathecal contrast density. Specifically, by placing a patient in decubitus Trendelenburg position with the head below the shoulders, contrast is likely to spread into the intracranial subarachnoid space, thus reducing the attenuation of the spinal subarachnoid space. In our static protocol, however, care is taken to keep the head above the shoulders, creating a trough of concentrated, dependently layering contrast in the thoracic spine, and limiting intracranial spread[6,16]. Also, their first acquisition was performed a little over 10 seconds after elevating the patient's hips, which could mean many first passes represented images within the first seconds of contrast having reached the CVF level, which might not have given enough time for the draining vein to adequately fill with contrast. This also differs from our dominant protocol, in which we scout the patient after elevation of their hips, usually meaning at least 1-2 minutes of interval between hip elevation and image acquisition.

We have found low false negative rates for acquisitions with highly dense intrathecal contrast, as low as 7% and 5% for series with thecal sac attenuation of over 1000 HU and 2000 HU respectively. Acquisitions with low attenuation of the thecal sac, on the other hand, had high rates of inconspicuous CVFs. For example, 67% of acquisitions with thecal sac attenuation under 1000 HU were falsely negative. These or similar thresholds could be used to drive decision-making intraprocedurally, by evaluating which levels might still benefit from

repositioning and rescanning (in our dominant protocol, static decubitus, patient repositioning is the main determinant of the location of the contrast bolus and thus the density of a given spinal level[16]). Also, for repeat examinations when a CVF has still not been found, the side and the levels that should be focused on might be chosen by inspecting which levels had inferior attenuation on previous negative CTMs. Furthermore, future research investigating improvements in CTM protocol could use attenuation values and previously determined attenuation benchmarks as surrogate endpoints whenever direct comparison of diagnostic yield is not possible.

Other factors aside from density and time probably play a role in the conspicuity of CVFs. Differences in breathing, for example, have been shown to dynamically increase or decrease CVF visibility[18,19]. In fact, in our study, even very high-density images were occasionally negative, which could be related to these variations.

Our study has limitations. First, the study cohort was relatively small. Even though the findings were significant, future studies with larger cohorts at other institutions are warranted to confirm the generalizability of our findings, especially under different acquisition protocols. Second, the qualitative visibility of the fistulas on each acquisition was evaluated by a single radiologist (DGLE), who was not blinded to its level. This subjective outcome would be best accessed by 2 blinded readers, which we encourage be done in further research. However, the findings relative to the subjective visibility of the CVF were confirmed by the objective opacification of its corresponding draining vein. Additionally, CVFs were only labeled as visible if findings were considered unequivocal. Classification of equivocal acquisitions, on the other hand, were more subjective, and categorization might vary if read by other radiologists. Third, the dominant acquisition protocol in our study was static decubitus, which differs significantly from ultrafast/dynamic ones (including DSM protocols). One should not interpret our findings to mean that time does not play a role in the conspicuity of CVFs, which it probably does, especially under dynamic protocols, only that this dependency probably mostly reflects density as a function of time. Fourth, the classification of the myelographic protocols was performed on an examination level, not for each acquisition, which means delayed acquisitions with diluted contrast were often present in ultrafast/dynamic and static decubitus examinations as well, but this should not interfere with the conclusions of this study, as acquisitions were compared separately regarding each variable, and comparing different examination protocols was not in our scope.

CONCLUSIONS

We have demonstrated a strong positive relationship between contrast density within the adjacent subarachnoid space and the conspicuity of CVFs. The timing of imaging acquisition after intrathecal injection of contrast was not an independent predictor of CVF visibility in our population. Density thresholds for minimal thecal sac contrast density could be used to evaluate the adequacy of acquisitions under the LDCTM protocol presented here.

REFERENCES

1. Kranz PG, Gray L, Malinzak MD, et al. CSF-Venous Fistulas: Anatomy and Diagnostic Imaging. *AJR Am J Roentgenol* 2021;217:1418–29.

2. Cheema S, Anderson J, Angus-Leppan H, et al. Multidisciplinary consensus guideline for the diagnosis and management of spontaneous intracranial hypotension. *J Neurol Neurosurg Psychiatry* 2023;94:835–43.

3. Lützen N, Demerath T, Würtemberger U, et al. Direct comparison of digital subtraction myelography versus CT myelography in lateral decubitus position: evaluation of diagnostic yield for cerebrospinal fluid-venous fistulas. *J NeuroIntervent Surg* https://doi.org/10.1136/jnis-2023-020789.

4. Schievink WI, Maya MM, Moser FG, et al. Lateral decubitus digital subtraction myelography to identify spinal CSF–venous fistulas in spontaneous intracranial hypotension. https://doi.org/10.3171/2019.6.SPINE19487.

5. Huynh TJ, Parizadeh D, Ahmed AK, et al. Lateral Decubitus Dynamic CT Myelography with Real-Time Bolus Tracking (dCTM-BT) for Evaluation of CSF-Venous Fistulas: Diagnostic Yield Stratified by Brain Imaging Findings. *American Journal of Neuroradiology* 2024;45:105–12.

6. Gibby JT, Amrhein TJ, Young DS, et al. Diagnostic Yield of Decubitus CT Myelography for Detection of CSF-Venous Fistulas. *American Journal of Neuroradiology* https://doi.org/10.3174/ajnr.A8330.

7. Kim DK, Carr CM, Benson JC, et al. Diagnostic Yield of Lateral Decubitus Digital Subtraction Myelogram Stratified by Brain MRI Findings. *Neurology* 2021;96:e1312–8.

8. Mark I, Madhavan A, Oien M, et al. Temporal Characteristics of CSF-Venous Fistulas on Digital Subtraction Myelography. *AJNR Am J Neuroradiol* 2023;44:492–5.

9. Callen AL, Fakhri M, Timpone VM, et al. Temporal Characteristics of CSF-Venous Fistulas on Dynamic Decubitus CT Myelography: A Retrospective Multi-Institution Cohort Study. *AJNR Am J Neuroradiol* 2023;45:100–4.

10. Headache Classification Committee of the International Headache Society (IHS) The International Classification of Headache Disorders, 3rd edition. *Cephalalgia* 2018;38:1–211.

11. Madhavan AA, Brinjikji W, Cutsforth-Gregory JK, et al. Myelographic Techniques for the Localization of CSF-Venous Fistulas: Updates in 2024. *American Journal of Neuroradiology* https://doi.org/10.3174/ajnr.A8299.

12. Madhavan AA, Verdoorn JT, Shlapak DP, et al. Lateral decubitus dynamic CT myelography for fast cerebrospinal fluid leak localization. *Neuroradiology* 2022;64:1897–903.

13. Mamlouk MD, Ochi RP, Jun P, et al. Decubitus CT Myelography for CSF-Venous Fistulas: A Procedural Approach. *American Journal of Neuroradiology* 2021;42:32–6.

14. Callen AL, Timpone VM, Schwertner A, et al. Algorithmic Multimodality Approach to Diagnosis and Treatment of Spinal CSF Leak and Venous Fistula in Patients With Spontaneous Intracranial Hypotension. *AJR Am J Roentgenol* 2022;219:292–301.

15. Kranz PG, Gray L, Amrhein TJ. Decubitus CT Myelography for Detecting Subtle CSF Leaks in Spontaneous Intracranial Hypotension. *AJNR Am J Neuroradiol* 2019;40:754–6.

16. Edelmuth DGL, Leão RV, Filho EN, et al. Safety and technical performance of bilateral decubitus CT myelography using standard versus increased intrathecal iodinated contrast volume. *American Journal of Neuroradiology* https://doi.org/10.3174/ajnr.A8436.

17. Kim DK, Brinjikji W, Morris PP, et al. Lateral Decubitus Digital Subtraction Myelography: Tips, Tricks, and Pitfalls. *AJNR Am J Neuroradiol* 2020;41:21–8.

18. Amrhein TJ, Gray L, Malinzak MD, et al. Respiratory Phase Affects the Conspicuity of CSF–Venous Fistulas in Spontaneous Intracranial Hypotension. *American Journal of Neuroradiology* 2020;41:1754–6.

19. Kranz PG, Malinzak MD, Gray L, et al. Resisted Inspiration Improves Visualization of CSF-Venous Fistulas in Spontaneous Intracranial Hypotension. *American Journal of Neuroradiology* 2023;44:994–8.

SUPPLEMENTAL FILES

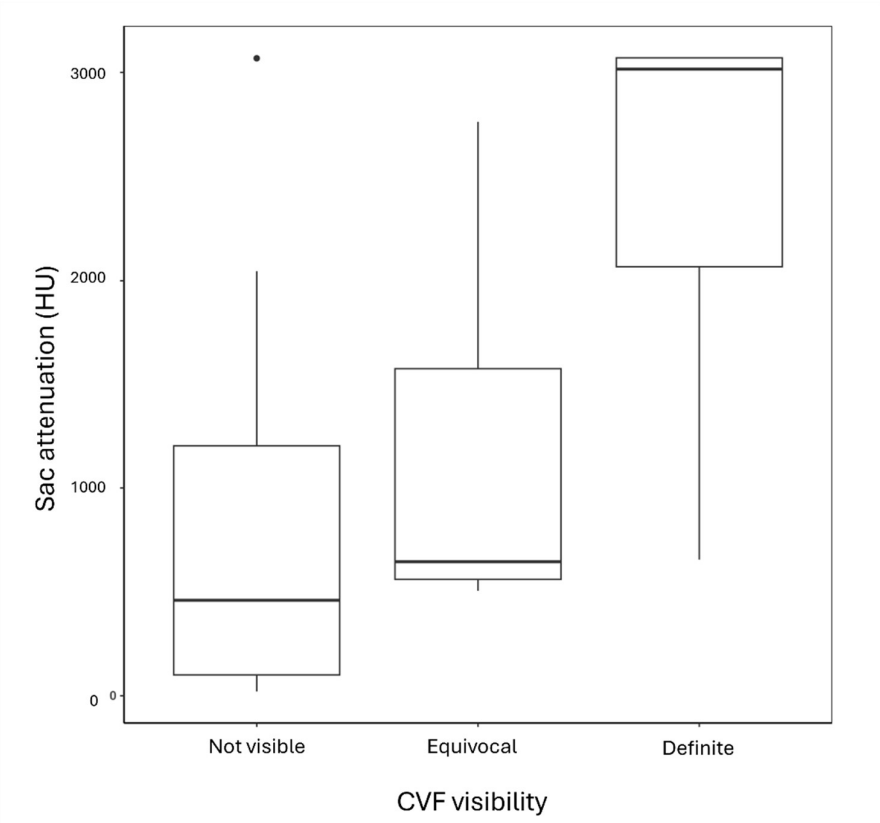

1. Boxplot graph showing the distribution of thecal sac contrast density in each group of CVF visibility when only considering acquisitions with the patient in ipsilateral decubitus to the CVF. The group with visible CVF showed a marked and statistically significantly higher mean density than the other two groups.

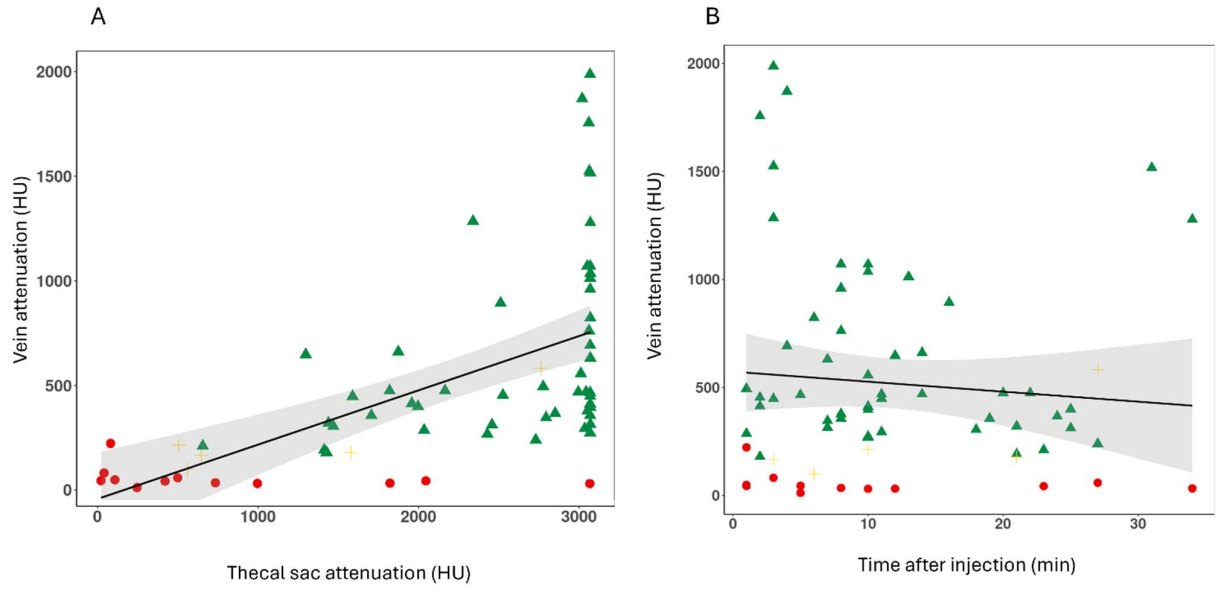

2. Considering only acquisitions with the patient in ipsilateral decubitus to the CVF. The y axis in both images represents the density of the draining vein of the known CVF. Each dot represents a CTM acquisition. Colors represent the subjective visibility of the CVF on that acquisition. In A, the x axis denotes the thecal sac attenuation on the level of a known CVF, with a statistically significant relationship, even after multivariate regression analysis correcting for time and position. In B, the x axis denotes the time passed between contrast injection and the acquisition, without a significant relationship to the density of the vein, before and after multivariate regression

correction. Relationship between time and vein attenuation is even smaller, as these acquisitions more frequently represent static decubitus protocol acquisitions, and less frequently delayed prone or supine acquisitions.

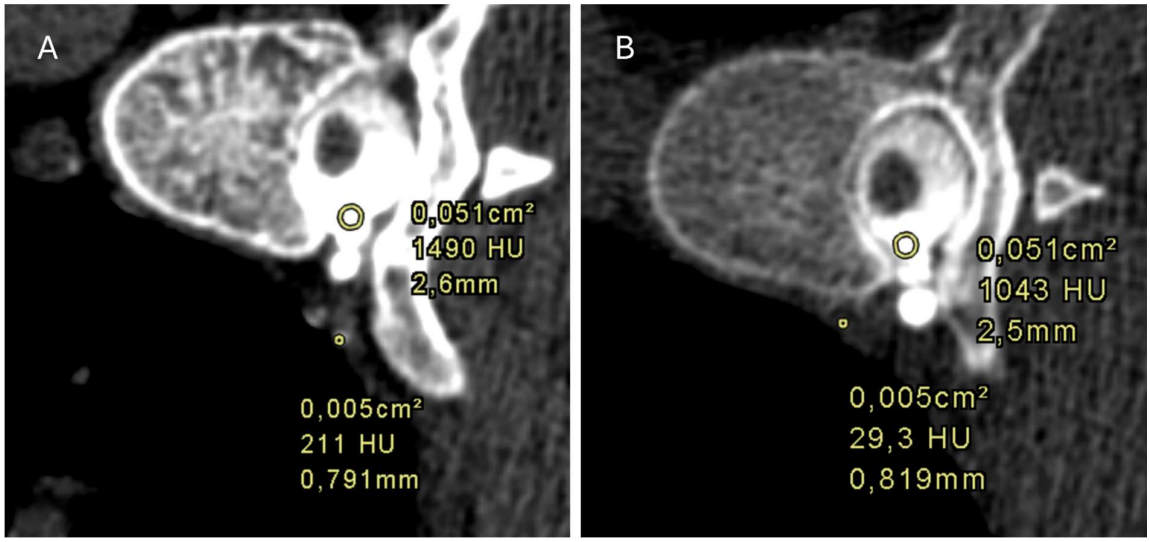

3. Two examples of thecal sac and vein attenuation measurements in two acquisitions during the same static decubitus CTM. In A, a definite CVF is noted by opacification of paraspinal veins up to the azygous vein. The point of most conspicuous venous contrast uptake is measured. In B, no signs of venous enhancement is seen, so the paraspinal vein of the corresponding level is measured.